International Journal of Robotics and Control Systems
Vol. 4, No. 4, 2024, pp. 1694-1711
ISSN 2775-2658
http://pubs2.ascee.org/index.php/ijrcs

Sensorless Speed Estimation Basing on MRAS Model for a PMSM Machine Application

Mohamed F. Elnaggar [a,b,1,*], Flah Aymen [b,c,d,e,f,g], Dina Mourad [a,h]

[a] Department of Electrical Engineering, College of Engineering, Prince Sattam Bin Abdulaziz University, Al-Kharj11942, Saudi Arabia
[b] Department of Electrical Power and Machines Engineering, Faculty of Engineering, Helwan University, Helwan 11795, Egypt
[c] Energy Processes Environment and Electrical Systems Unit, National Engineering School of Gabès, University of Gabes, Gabes, 6029, Tunisia
[d] MEU Research Unit, Middle East University, Amman, 11831, Jordan
[e] University of Gabès, Private Higher School of Applied Sciences and Technology of Gabès, Gabes, 6029, Tunisia
[f] Applied Science Research Center, Applied Science Private University, Amman, 11931, Jordan
[g] University of Business and Technology (UBT), College of Engineering, Jeddah 21448, Saudi Arabia
[h] Faculty of Technology and Industrial Education, Helwan university, Cairo, Egypt
[1] mfelnaggar@yahoo.com
* Corresponding Author

ARTICLE INFO

Article history
Received August 05, 2024
Revised September 13, 2024
Accepted October 14, 2024

Keywords
Sensor;
Controller;
PMSM;
Speed Estimation;
High-Speed Estimation;
MRAS Algorithm;
Wind Energy Systems

ABSTRACT

Wind energy systems utilizing synchronous machines can encounter challenges with speed detection at high rotational speeds due to increasing motor temperatures affecting parameters like stator resistance. This paper addresses these challenges by proposing a novel high-speed estimator algorithm based on the Model Reference Adaptive System (MRAS) approach. The primary contribution of this research is the development of an MRAS-based speed estimator that leverages a reactive power model to maintain robustness against variations in stator resistance, even at elevated speeds. To optimize the estimator's performance, we employed a particle optimization algorithm for tuning, which overcomes issues related to regulator parameter identification. We implemented the proposed algorithm in Matlab and validated it on a real machine prototype capable of high-speed operation. After a comparison wth 5 different methods, the results indicate that the estimator performs effectively up to 42,000 RPM (600 Hz), demonstrating a maximum speed estimation error of 50 Hz. Stability analyses across various speed regions and practical lab tests confirm the robustness and accuracy of the proposed control scheme. The findings highlight the estimator's improved performance in high-speed scenarios, showcasing its potential for enhancing speed detection in wind energy systems.

1. Introduction

1.1. Research Background

Wind energy systems, particularly hybrid wind setups, rely heavily on electrical motors for efficient torque generation and system acceleration. Various motor types, including Direct Current (DC) motors, Brushless AC and DC motors, Interior Permanent Synchronous Motors (IPMSM),

Permanent Synchronous Motors (PMSM), and Switched Reluctance Motors, are employed in these systems [1], [2]. A comparative analysis detailed in [3] highlights that the Permanent Magnet Synchronous Machine (PMSM) is favored for its broad power range and high power density, making it the most efficient choice for wind energy applications [4], [5]. Selecting the appropriate motor type is essential for making a robust and efficient wind energy production system, but monitoring this motor with the best functioning is a surely important objective. In the majority of research works, induction motors can be operated by two essential strategies, the first being the vector control method and the second being the direct torque control method. Each method presents its advantages and disadvantages. Selecting the optimal motor type is crucial for the efficiency and robustness of wind energy systems. Motor control strategies such as Vector Control and Direct Torque Control are commonly employed. Vector Control, noted for its simplicity and adaptability across various applications, is particularly relevant for high-performance wind energy systems [6]-[8]. This paper focuses on enhancing motor speed control through Vector Control to improve system performance under dynamic external conditions.

1.2. Research Gap and Problem Statement

The research gap identified in this study revolves around the limitations of current speed estimation methods for Permanent Magnet Synchronous Motors (PMSMs) operating at high speeds [6]-[8]. Traditional methods, including rotary encoders and resolvers, face significant challenges such as high costs, size constraints, and sensitivity to external factors like dust and temperature, which can compromise system robustness and reliability. Additionally, existing sensorless speed estimation techniques, such as those based on Model Reference Adaptive Systems (MRAS), have demonstrated limited robustness and effectiveness specifically in high-speed operational ranges [9]-[13]. The primary goal of this research is to develop a more reliable and cost-effective speed estimation solution that can operate efficiently at high speeds. The proposed solution aims to overcome the limitations of conventional methods by introducing a robust MRAS-based estimator enhanced with Particle Swarm Optimization (PSO) [14]-[16]. This new approach is designed to maintain high performance and accuracy even in the challenging conditions of high-speed operation [17], [18]. By addressing these gaps, the research contributes significantly to advancing the state-of-the-art in motor control for wind energy systems. It offers a novel solution to the problem of accurate speed estimation at high velocities, which is crucial for improving the efficiency and robustness of PMSM drive systems in practical applications.

1.3. Proposed Solution and Novelty

To address these challenges, recent advancements suggest the use of software-based speed encoders as a viable alternative. This paper proposes a robust software speed encoder using the Model Reference Adaptive System (MRAS) technique, designed to operate effectively at high speeds. Existing literature shows that sensorless speed estimation methods like MRAS have limitations in high-speed conditions [10]-[12]. Our proposed approach enhances MRAS with a Particle Swarm Optimization (PSO) algorithm to address limitations related to parameter adaptation and system nonlinearity [13]-[16].

1.4. Research Contributions

The research contributions are twofold: First, the paper introduces a novel MRAS-based speed estimator that maintains robustness at high operational speeds, addressing a critical gap in existing sensorless methods. Second, it integrates Particle Swarm Optimization into the MRAS framework to improve estimator accuracy and adaptability. This work provides a significant advancement in high-speed motor control, offering a more reliable and cost-effective solution for wind energy systems.

1.5. Paper Organization

This paper is structured as follows: Section 2 explores the field weakening phenomenon and its implications for high-speed motor operation. Section 3 details the principles of the proposed speed observer and MRAS-based estimator. Section 4 presents the stability analysis, while Section 5

discusses the experimental results and their implications. Finally, Section 6 concludes with a summary of findings and recommendations for future research.

2. Permanent Magnet Machine: Design and Modelling

As the application model is based on the induction machine, the corresponding electrical machine needs to be identified and mathematically understood in the case of the wind system. Motor. As explained in the introduction section, high-speed control is vital to this application. In the nominal situation, increasing the stator input voltage over the nominal one is impossible for operating at a high speed. This condition corresponds to the nominal speed of the motor running. The plan is to find the best control method and ensure motor security and speed goals. Based on our previous study, the concept of field weakening can be operated to resolve the high-speed running phenomenon [6].

The idea behind this technology is comparable to that of a DC machine, in which the flux can be controlled separately. Therefore, achieving a high-speed region requires flux minimization. The flux generated by the rotor magnet (λm) is the issue that has emerged, making it challenging to minimize the overall motor flux. Generally speaking, maintaining zero direct stator current ensures the rated speed mode. The direct flux component must be decreased to influence the high-speed mode, according to the flux formulas shown in (1). Lowering the direct stator component to the negative zone will ensure this action [19]-[21].

$$\begin{cases} I_d^2 + I_q^2 \le I_{max}^2 \\ V_d^2 + V_q^2 \le V_{max}^2 \end{cases} \quad (1)$$

The issue that has emerged during this phase has to do with the theory that is required to generate the requisite direct stator current in order to ensure that this running mode is safe. The concept relates to voltages and currents that are less than a maximum. The limit system of equations takes into consideration the maximum voltage and maximum current, as stated in [22] which is typically determined by the inverter. The maximum inverter phase-current and phase-voltage amplitudes are represented by the values Imax and Vmax, respectively.

These limit equations allow for the field weakening zone to be utilized. Two different kinds of circles—one for the voltage limitation condition and one for the current limitation—are shown in Fig. 1 [23]. The speed inverses determine the voltage limitation's radius. In actuality, the voltage circle radius shrinks as speed rises. Additionally, the PMSM settings determine the voltage circle center.

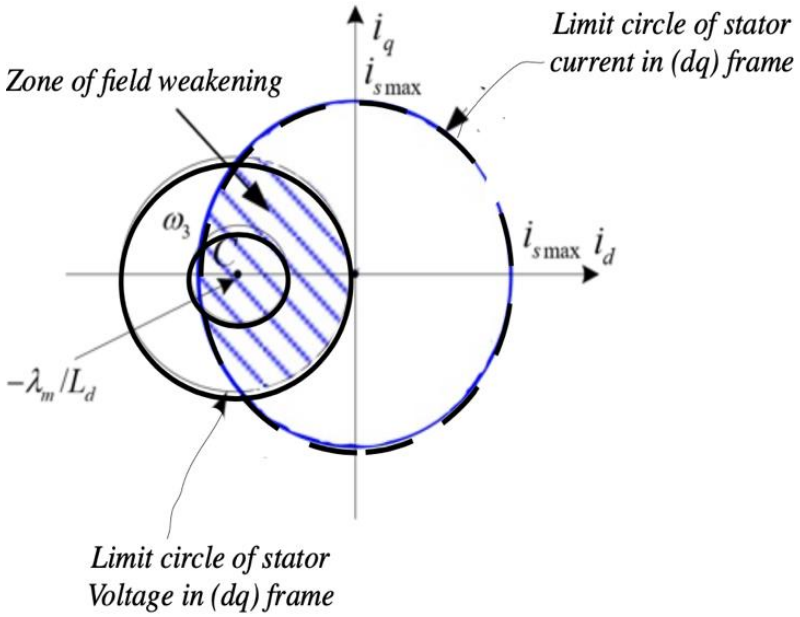

Fig. 1. Diagram of a field weakening plan

As a first step, it is mandatory to try to express the related stator current expression in the "direct" component, as it is the only variable that can be used to decrease the flux inside the machine.

Equation (3) exposes this expression. This relation was depicted from the voltage equation model as it is presented in equation (2). So, if supposing that the saturation effect is null and if supposing that the hysteresis iron loss is absent, it will be able to expose the high-speed control loop, which will calculate the necessary direct stator current component as it is in Fig. 2 [24], [25].

$$\begin{bmatrix} v_d \\ v_q \end{bmatrix} = \begin{bmatrix} R_s + pL_d & -\omega L_d \\ \omega L_d & R_s + pL_q \end{bmatrix} \begin{bmatrix} i_d \\ i_q \end{bmatrix} + \begin{bmatrix} 0 \\ \omega \lambda_m \end{bmatrix} \tag{2}$$

$$i_d^* = \frac{\sqrt{V_{max}^2 - (\omega L_q i_q)^2} - \omega \lambda_m}{\omega L_d} \tag{3}$$

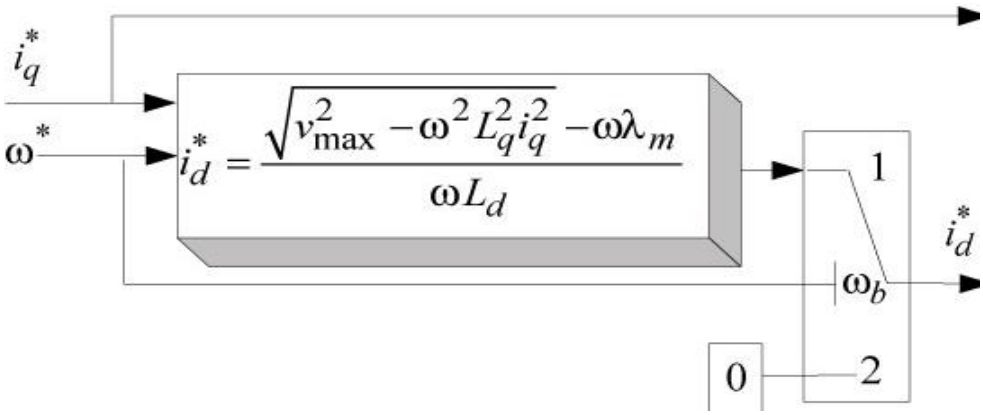

Fig. 2. High-speed algorithm (HSA)

This block is incorporated into the vector control algorithm to generate the necessary stator voltage. Following the speed controller block, the quadrature reference current is obtained, and the HAS algorithm calculates the direct stator current. We can generate the reference stator voltages using two more Pi controls.

3. MRAS-Reactive Power Speed Observer Design

The Model Reference Adaptive System (MRAS) is a sophisticated technique employed for rotor speed estimation in Permanent Magnet Synchronous Motors (PMSMs), particularly advantageous in high-speed applications. The core of the MRAS approach lies in its dual-model structure, consisting of a reference model and an adaptive model. The reference model is designed based on the theoretical understanding and desired performance of the motor system, representing an idealized motor behavior. In contrast, the adaptive model simulates the real motor dynamics, incorporating actual operating conditions and variations in motor parameters such as stator resistance and magnetic flux. The MRAS algorithm functions by continuously comparing the outputs of these two models and adapting the parameters of the adaptive model to minimize the discrepancy between the observed and reference behaviors. This adaptation process involves using a proportional-integral (PI) controller or other similar mechanisms to refine the model parameters dynamically.

A key enhancement in MRAS for PMSM speed estimation is the incorporation of the reactive power model. Reactive power, which oscillates between the source and the motor without contributing to real work, is intricately linked to the rotor speed and the motor's magnetic characteristics. By employing the reactive power model, the MRAS estimator can leverage reactive power measurements—obtained from the motor's voltage and current data—to provide insights into rotor speed [26], [27]. This model is particularly valuable in addressing the challenges associated with high-speed operation where traditional methods may falter. The reactive power-based MRAS estimator

calculates the reactive power from motor measurements and uses this information to estimate the rotor speed, compensating for variations in motor parameters and load conditions.

Those, the efficiency of this estimation methodology is used. This method can be considered the most proficient when compared to the Back-Emf and state observer methods [28]. Some authors link this one to intelligent estimating techniques in other literature, where fuzzy and neural solutions may also be appealing. Nevertheless, these systems' drawbacks are the need to understand database information [29]-[31]. As a result, the majority of published research based on techniques made use of mathematical models like MRAS, Lunberger, etc., and the outcomes demonstrate the effectiveness of the suggested solutions in [16]-[18].

The "reference and adjustable models" mathematical models, which are shown in Fig. 3, form the foundation of the MRAS principle (3). The results will be contrasted and applied to a certain algorithm in order to determine or approximate a specified parameter. This output signal is typically utilized in the adjustable model as well. The issue with the MRAS estimator has to do with the stability phenomena, which can cause the global system to become unstable if the mechanisms for adaptation and adjustment are not carefully chosen and identified. It is possible to fix this issue using Popov's Hyper Stability Criterion.

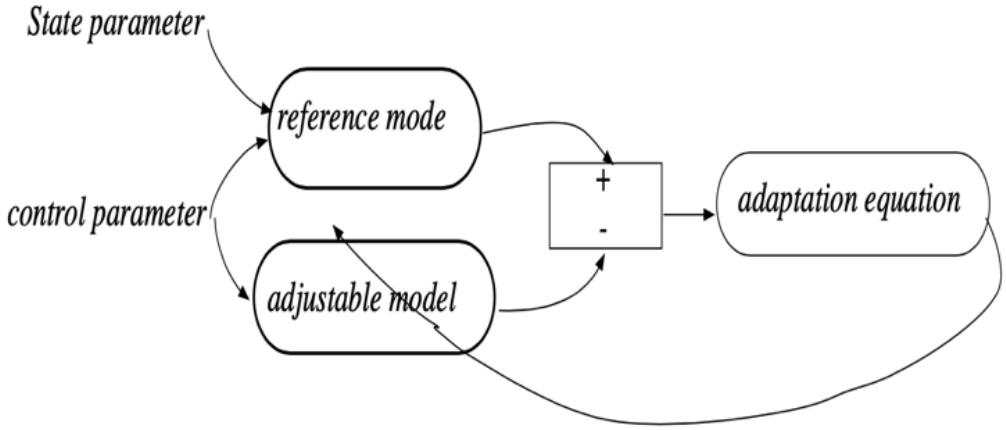

Fig. 3. General design of the model reference adaptive system

In relation to the desired application specification, the PMSM machine speed will be estimated online, as the main objective is to replace the mechanical speed encoder with the software application. So, as a first work step, the adaptable mathematical model needs to be built and formed by using the different previous equations. However, if referring to the literature, more than one type of MRAS observer can be applied as the Back-EMF (E-MRAS), reactive power (Q- MRAS) and active power (AMRAS). However, the selection of the best solution depends on knowing the specifications of the interior machine design. Here, each selected MRAS model has its advantages and drawbacks.

If concentrating on the related cited works as is in [12] and [18], some standard MRAS estimators have a sensitivity to some parameters variation as the stator resistance. This parameter is depending the electrical motor's existing temperature. Even if the temperature is high, the stator resistance changes and this can make the esteemed parameters, such as the stator resistance value, wrong and different from the reality. Therefore, the present model has an advantage over other exposed solutions in the cited references, where the proposed solution is independent from that parameter. In relation to high speed mode, where the high speed comes with a high temperature, Increasing the motor temperature might result in an increase in the motor stator resistance value. It seems that the exposed Q-MRAS resolves this issue. Starting with the basing relation of the reactive power, as it is in equation (4);

$$Q_s = v_q i_d - v_d i_q \tag{4}$$

if based on what is exposed previously on the stator voltages, the reactive power expression can be formulated as it is in equation (5).

$$Q_s = \omega\left(L_d i_d^2 + L_q i_q^2\right) + \left(L_d i_d^2 \frac{di_q}{dt} - L_q i_q \frac{di_q}{dt}\right) + \omega i_d \lambda_m \quad (5)$$

In the permanent regions, where the torque and the motor speeds are constant then, it is possible to migrate equation (5) to what is in equation (6), where all currents can be supposed to be constant.

Basing the stator currents as the direct and transversal components, the adjustable Q-MRAS model is illustrated in equation (7).

$$Q_s = \omega\left(L_d i_d^2 + L_q i_q^2\right) + \omega i_d \lambda_m \quad (6)$$

$$\widehat{Q_s} = \hat{\omega}\left(L_d \hat{i}_d^2 + L_q \hat{i}_q^2\right) + \hat{\omega}\hat{i}_d \lambda_m \quad (7)$$

When the real and the esteemed reactive power are confirmed, the adaptation protocol is built. The related graph is exposed in Fig. 4 [32].

If using the two equations (4) and (7) and after doing a subtraction action, equation (8) can explain the power error value and the overall reactive power generated from the MRAS estimator. The related scheme is exposed in Fig. 4 [11], [33].

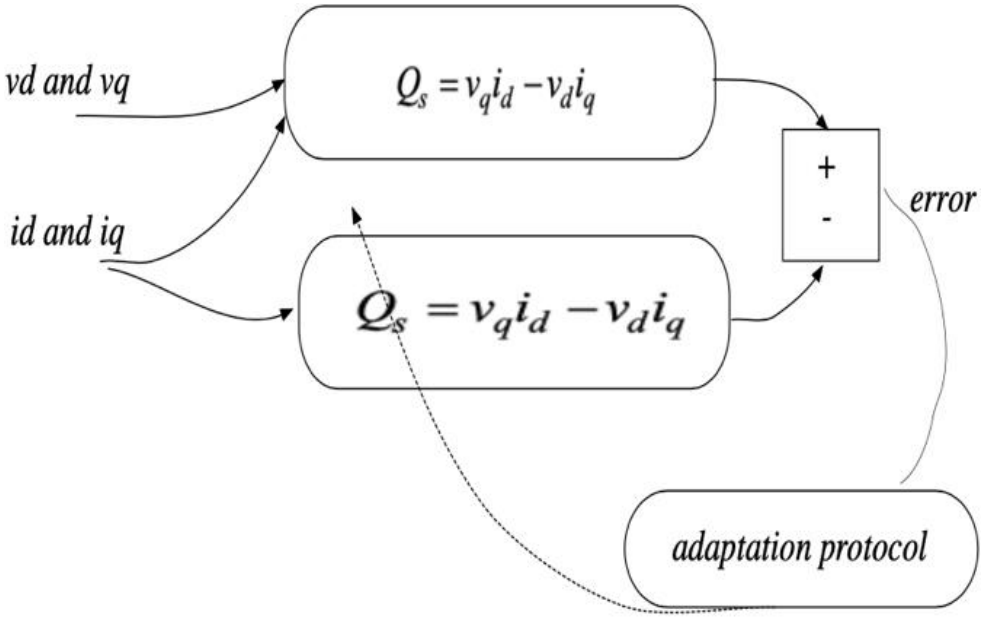

Fig. 4. Reactive MRAS power adaptation mechanism

$$e_q = Q_s - \widehat{Q_s} = v_q i_d - v_d i_q - \left(L_d \hat{i}_d^2 + L_q \hat{i}_q^2\right) - \hat{\omega}\hat{i}_d \lambda_m = \alpha + \hat{\omega}\beta \quad (8)$$

The primary advantage of the MRAS-reactive power speed observer is its robustness and accuracy. The reactive power model enhances the estimator's ability to remain accurate even when motor parameters change or under varying operational conditions. This robustness is crucial in high-speed scenarios where conventional speed sensors may be impractical due to size, cost, or sensitivity issues. The adaptive nature of the MRAS algorithm allows it to adjust continuously to parameter variations, maintaining high estimation accuracy despite potential disruptions or changes in motor characteristics.

The MRAS-reactive power speed observer thus represents a significant advancement in motor control technology. It provides a reliable alternative to traditional speed sensors by offering accurate speed estimation through adaptive modeling and reactive power analysis. This approach is particularly beneficial in applications where maintaining performance at high speeds is critical, such as in advanced wind energy systems and other high-performance motor-driven applications [34], [35]. By

improving the accuracy and robustness of speed estimation, the MRAS-reactive power method contributes to enhanced control and efficiency in PMSM systems, marking a substantial improvement over conventional estimation techniques.

Firstly, it is interesting to decompress the system of equations as it is in Fig. 5. So, the POPV hyperstability condition can be validated and confirmed.

The working principle of the adaptation mechanism is based on the POPOV conditions. Firstly, it is mandatory to verify that the linear model is strictly positive. The second POPOV condition is supposed to have a nonlinear model which satisfies the inequality expressed in (10). Then, it is possible to validate the adaptation mechanism.

Based on the POPOV theorem, the only related solution can be made if the sign bloc is adapted in the control loop. So, by using equation (11), the second stability condition is guaranteed. We mention by W as it is expressed here:

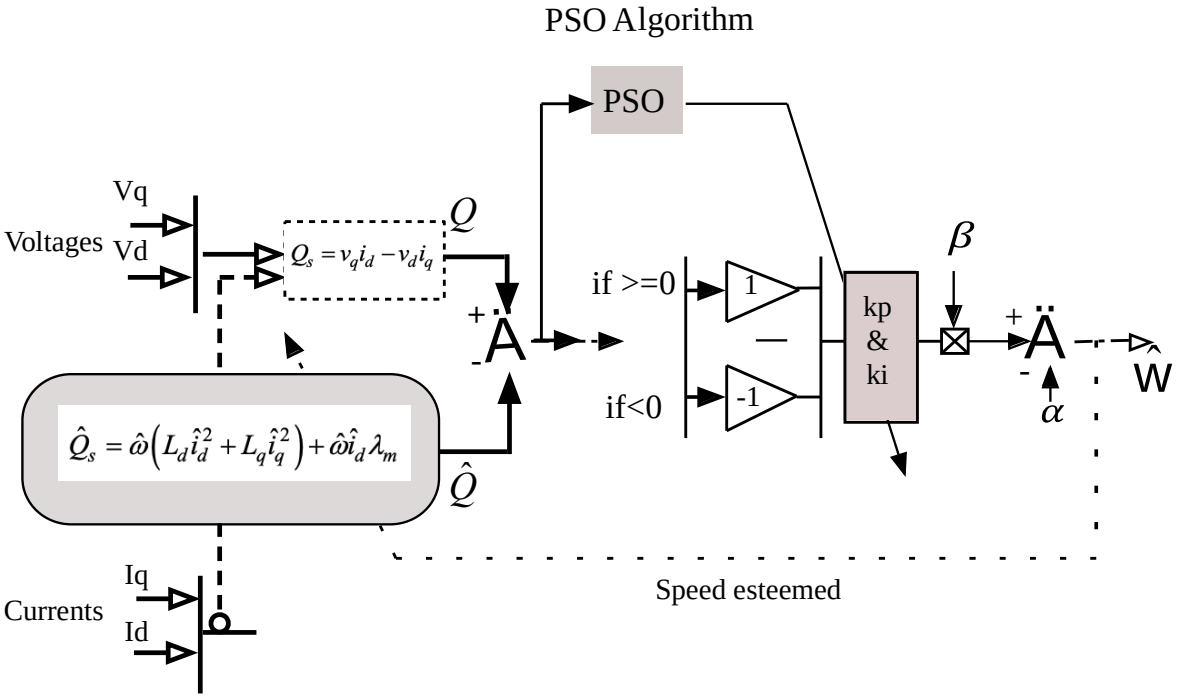

Fig. 5. Q-MRAS total structure improved by PSO algorithm

$$w = -\alpha - \hat{\omega}\beta \tag{9}$$

$$\int_0^t v^T(w)dt \geq -\gamma_0^2 \tag{10}$$

$$\begin{cases} \int_0^t v^T(-\alpha)dt \geq -\gamma_0^2 \\ \int_0^t v^T(-\hat{\omega}\beta)dt \geq -\gamma_1^2 \end{cases} \tag{11}$$

The first part of the system (11) is guaranteed due to lemma 1 [36],

Lemma 1

$$\alpha \leq 0 \Longrightarrow -\alpha \geq 0 \Longrightarrow \int_0^t v^T(-\alpha)dt \geq 0 \tag{12}$$

Also, by applying the lemma 2, The second part of the equation (11) will be justified.

Lemma 2

$$\begin{cases} v = D_{eq,} & D\ is\ the\ sign\ Bloc \\ \widehat{\omega} = (k_p + {k_i}/{s})v \end{cases} \tag{13}$$

4. Stability Analysis of the Reactive Power MRAS Estimator

The Q_MRAS scheme can be represented by this simple control loop, as presented in Fig. 6. The PI controller is used to adjust the speed of a G(s) system [38], [6], [39], [40].

Fig. 6. Simplify the control loop of Q_MRAS

Started identifying the necessary mathematical expressions:

The PI input signal is defined by the error between the real and the estimated reactive power as expressed as fellow [6], [41]:

$$e_q = Q_s - \widehat{Q_s} = v_q(i_d - \hat{\imath}_d) - v_d(i_q - \hat{\imath}_q) \tag{14}$$

We note by: $x = [i_d \quad i_q]$, $u' = [v_d \quad v'_q]$, $v'_q = v_q + w\frac{\lambda_m}{L_q}$

Refers to the previous error equation, the G(s) expression can be elaborated as indicated in equation (15).

$$\frac{e_q}{\Delta_w} = v_q\left(\frac{\Delta i_d}{\Delta_w}\right) - v_q\left(\frac{\Delta i_q}{\Delta_w}\right) = G(s) \tag{15}$$

Remained $\frac{\Delta i_d}{\Delta_w}$ and $\frac{\Delta i_q}{\Delta_w}$ are expressed in (20) and (21).

After checking all the necessary expressions, the closed loop formula can be obtained as indicated in equation (16).

$$\frac{w}{\widehat{w}} = \frac{G.(k_p + {k_i}/{s})}{1 + G.(k_p + {k_i}/{s})} \tag{16}$$

The demonstration of the presented equations is as follows:

Starting from the voltage equations expressed in (3), the system equation can be represented by:

$$\begin{cases} \dot{x} = Ax + Bu' \\ y = Dx \end{cases} \tag{17}$$

After applying the lesser variation on the stator current, the new system equations can be formulated as follows:

$$\begin{cases} \dot{\Delta x} = A\,\Delta x + \Delta A\, x_0 \\ \Delta y = D.\Delta x \end{cases} \tag{18}$$

We note by $\Delta A = \begin{bmatrix} 0 & \frac{L_q}{L_d} \\ \frac{-L_q}{L_d} & 0 \end{bmatrix}. \Delta w \; and \; by \; D = \begin{bmatrix} 1 & 0 \\ 0 & 1 \end{bmatrix}$

The new output variation expression becomes as it is in (19).

$$\Delta y = D(sI - A)^{-1} \Delta A \, x_0 \tag{19}$$

We mention by $\Delta y = \begin{bmatrix} \Delta i_d \\ \Delta i_q \end{bmatrix}. \Delta w \; and \; \mathrm{x}_0 = \begin{bmatrix} i_{d0} \\ i_{q0} \end{bmatrix}$

And

$$(sI - A)^{-1} = \frac{1}{\det(sI - A)} \begin{bmatrix} s + \frac{R_s}{L_d} & w\frac{L_q}{L_d} \\ -w\frac{L_q}{L_d} & s + \frac{R_s}{L_q} \end{bmatrix}$$

Then the expressions of the stator current variations are exposed in the system of equation (20) and (21):

The stability analysis was applied in different speed zones, starting from 5000 rpm and touching 42000 rpm, the maximum speed supported by the used motor. Fig. 7 presents the obtained Nyquist graph. The results show the stability of the speed observer under high-speed variation. These results guarantee the overall observed system stability.

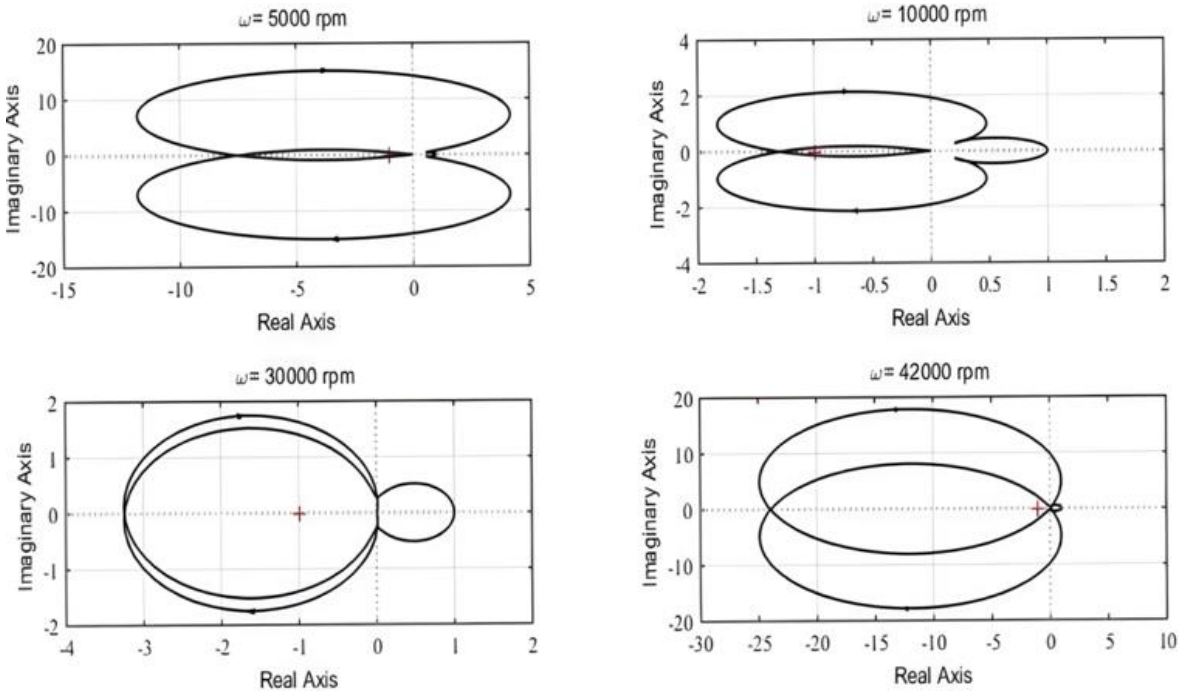

Fig. 7. Nyquist map for the Q_MRAS speed observer under different speeds

$$\frac{\Delta i_d}{\Delta w} = \left[-w\left(\frac{L_q}{L_d}\right)^2 i_{d0} + \left(s + \frac{R_s}{L_d}\right)\frac{L_q}{L_d} i_{q0} \right] \frac{1}{\det(sI - A)} \tag{20}$$

$$\frac{\Delta i_q}{\Delta w} = \left[-w\left(\frac{L_q}{L_d}\right)^2 i_{q0} - \left(s + \frac{R_s}{L_d}\right)\frac{L_q}{L_d} i_{d0} \right] \frac{1}{\det(sI - A)} \tag{21}$$

So, after cheeked the system G(s), the closed loop function can be represented by eq. (20).

$$H(s) = \frac{\beta k_p s^2 + (\alpha k_p + \beta k_i)s + \alpha k_i}{s^3 + s^2(2\frac{R_s}{L_d} + \beta k_p) + \gamma' s + \alpha k_i} \quad (22)$$

It is noted that the parameters:

$\gamma' = w^2 + (\alpha k_p + \beta k_i)$, $\zeta = (v_q i_{q0} + v_d i_{d0})$

$\zeta' = (v_d i_{q0} - v_q i_{d0})$,

And.

$$\begin{cases} \alpha = a\, b\, \zeta + \zeta' w\, b^2 \\ \beta = b\zeta \\ a = \frac{R_s}{L_d} \\ b = \frac{L_q}{L_d} \end{cases}$$

5. Description of the Experimental System and the System Blocs

In this section, we want to present the experimental bank used to validate the high-speed control loop. The global material group can be shown in Fig. 8. Basically, the Permanent magnet synchronous motor is related to a compressor system, which can reach a very high speed by injecting a high-pressure oil. This is for simulating the high-speed regions [42], [43]. The specifications of the used electrical machine can be summarized in the Table 1.

Table 1. Electrical machine parameters

Motor Type	2AML406B-090-10-170
Manufacture	VUES Brno
Nominal Speed	25 K rpm
Maximum speed	42 k rpm
Nominal current	11 A
Control strategy	FOC

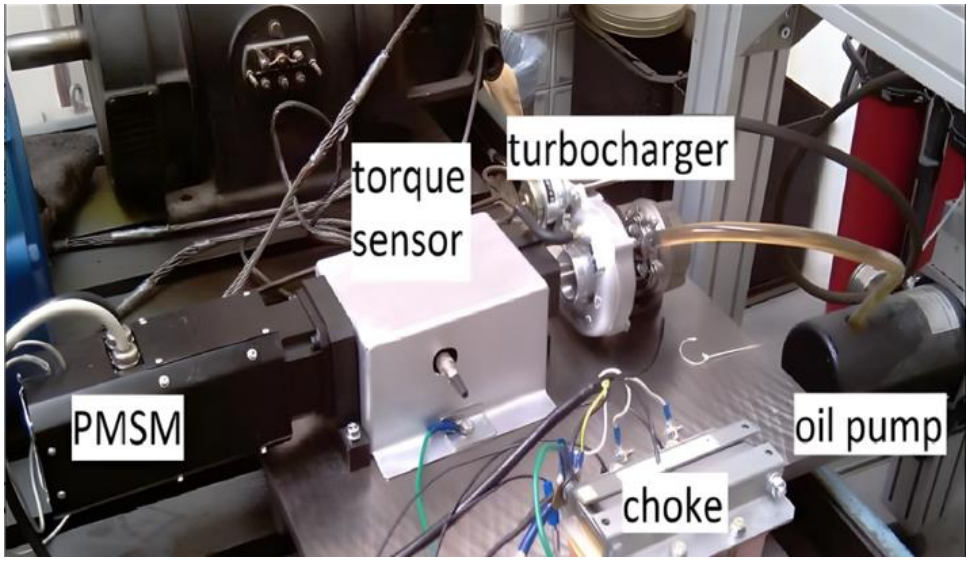

Fig. 8. Practice experiment tools

In this application, the load charge is a turbocharger related to an oil pump, and its load torque is equivalent to the load of one road used in a wind system, where this load torque decreases when the

speed rotation increases. The motor alimentation is from a three-phase inverter controlled by a DSP card throughout a PC.

The rectified voltage supplies an insulated gate bipolar transistor (IGBT) inverter. The inverter uses a power module SKM75GD124D and IGBT/MOSFET driver SKHI61, both from Semikron [44], [45].

In the hardware implementation, a vector control strategy coupled with the software speed encoder is used to control the machine. As explained in the previous section, the speed software encoder called Q-MRAS requests a lot of motor information, such as currents and tensions in the (d, q) frame. Those signals are obtained from ADC blocs inserted in the control card. In addition,

In the motor operation loop, the high-speed algorithm (HSA) is inserted to verify the global system performance [46]. Fig. 9 gives more explanation.

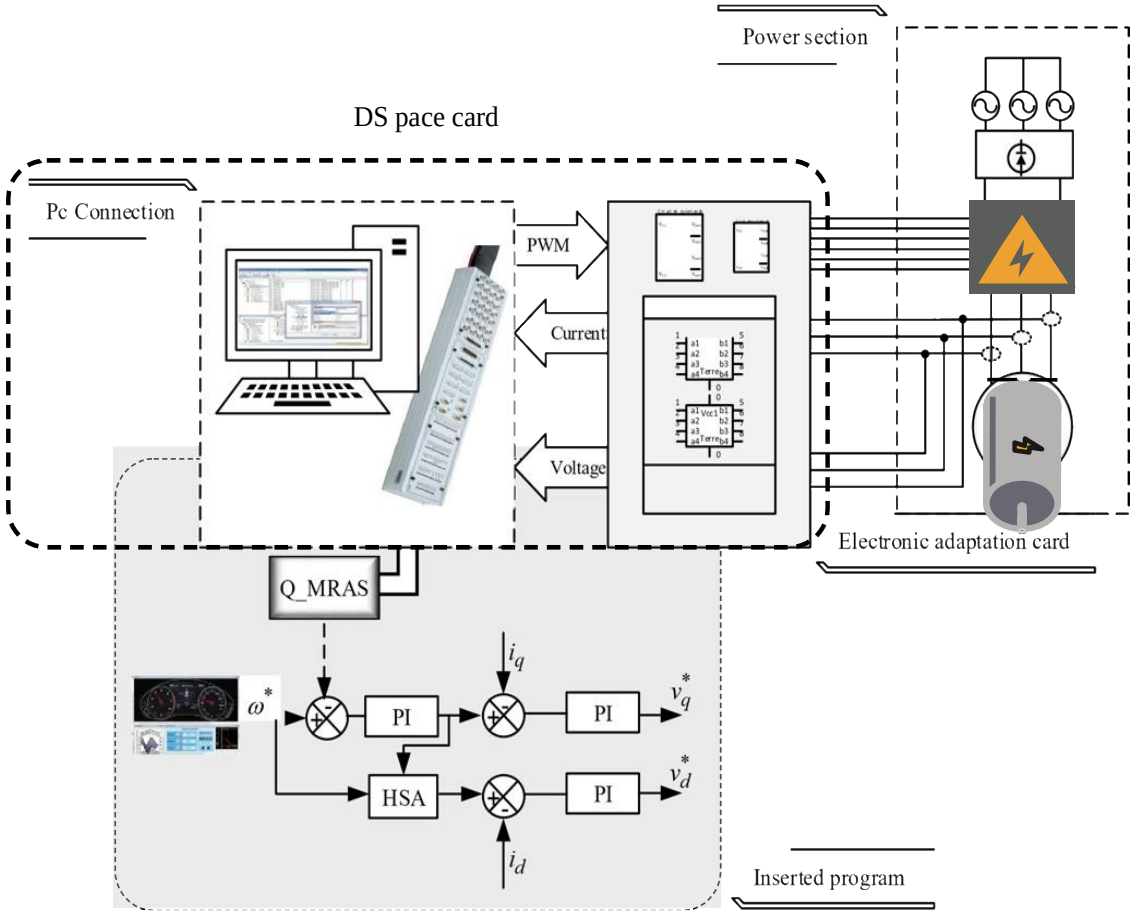

Fig. 9. Vector control strategy and relation to the overall system blocs

6. Results Exposition and Discussion

In this section, the obtained results are presented and analyzed, and the total system performance is tested and confirmed under high-speed operating conditions, taking into account the performance of a wind system's applied load. The experimental materials serve to test and validate the system's performance.

Because the vector control operation has been modified to control this prototype, it is necessary to adhere to the control strategy and verify that the corresponding current and voltage variables are in normal condition.

Fig. 10 illustrates the vector control method's fundamentals, with the direct current essentially negative. As a result, the vector principle and high-speed theory have been thoroughly verified. The

present ripples in those variables are due to the inverter model, which uses 15 Mhz as a commutation variable. If the inverter frequency exceeds 15 Mhz, there may be less ripples in these values.

The existing ripples are not related to the sole inverter specification, but rather to the commutation blocs introduced in the HAS and Q-MRAS. This demonstrates the flaws in this application's code.

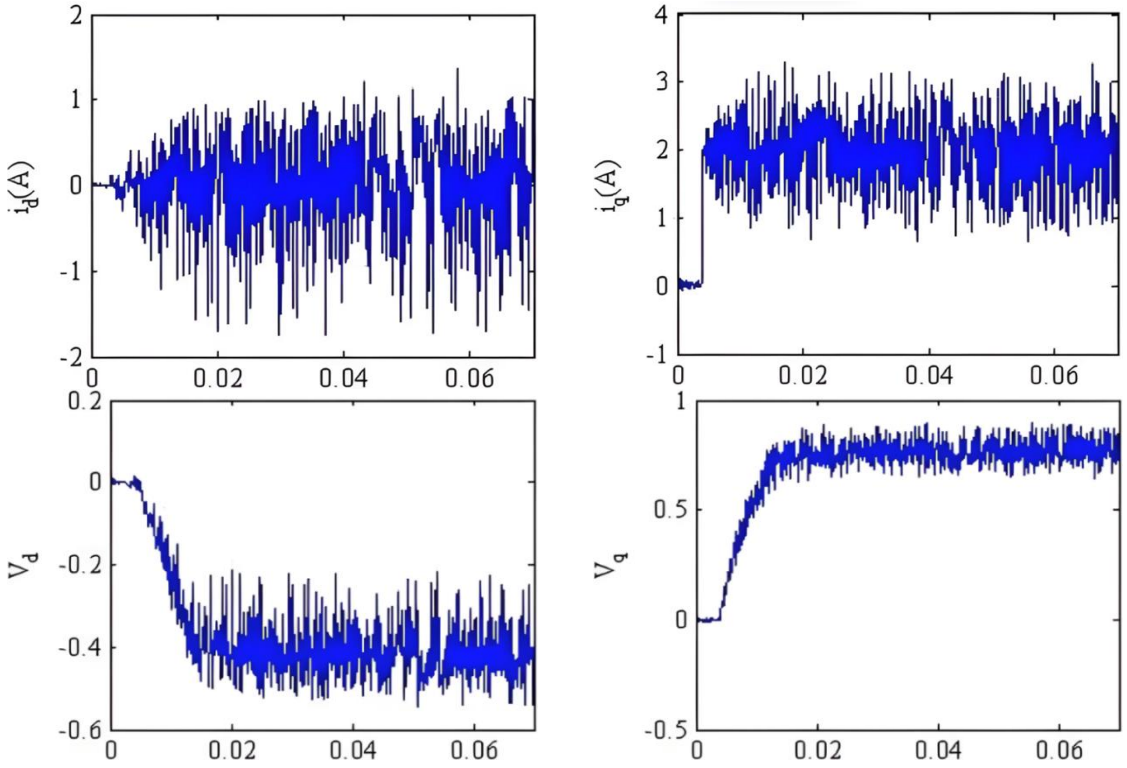

Fig. 10. Currents and voltage results

In parallel to these results, the algorithm feedback must concentrate on the given speed specification as shown in Fig. 11 and Fig. 12, which represent the obtained speed results and the obtained speed error.

Based on the given results, the efficiency of the proposed speed encoder is justified. However, it would be more interesting if it could be compared to other solutions in order to define the optimal solution.

Table 2, gives the performances of the proposed high-speed encoder for the case when Using an Interval Sliding Mode Observer [47], in [48], the High-Speed Motors Based on a Polarity Switching Tracking Filter and Disturbance Observer is used. an ameliorated A High-Speed Sliding-Mode Observer for the Sensorless Speed Control of a PMSM is also used in [49] and a second improved adaptive sliding mode speed observer is used in [50].

The comparison was based on error level for the high speed regions for a similar motor specification.

The exposed comparison demonstrates that the very high speed motor tests were not frequently applied to an extreme degree. However, even as the motor speed increases, the mistake moves on. The proposed speed estimator exhibits good behavior and an acceptable level error of 2.8% at a very high speed of 42K rpm.

For proving the efficiency of the proposed speed observer, the rest of this section will demonstrate the efficiency of the global loop performance which is applied under two conditions: the given reference speed is equivalent to 32000 rpm (650 HZ) and the given load torque decreases proportionally. At t=0.01 Te=1.2 Nm and at t=0.06 Te=1 Nm.

Table 2. Comparison face five different speed observer

Provider reference	Suggested Speed Sensor	Maximum speed	Estimation Erro
[51]	speed and load torque observers (LTO)	1326 rpm	2%
[50]	Adaptive Sliding mode (ASMO)	2000 rpm	1.2%
[49]	Modified SMO	3000 rpm	2%
[48]	Disturbance observer	8000 rpm	3%
[47]	Interval sliding mode	3000 rpm	3.5%
Proposed observer	Q-MRAS	32000 rpm	2.8%

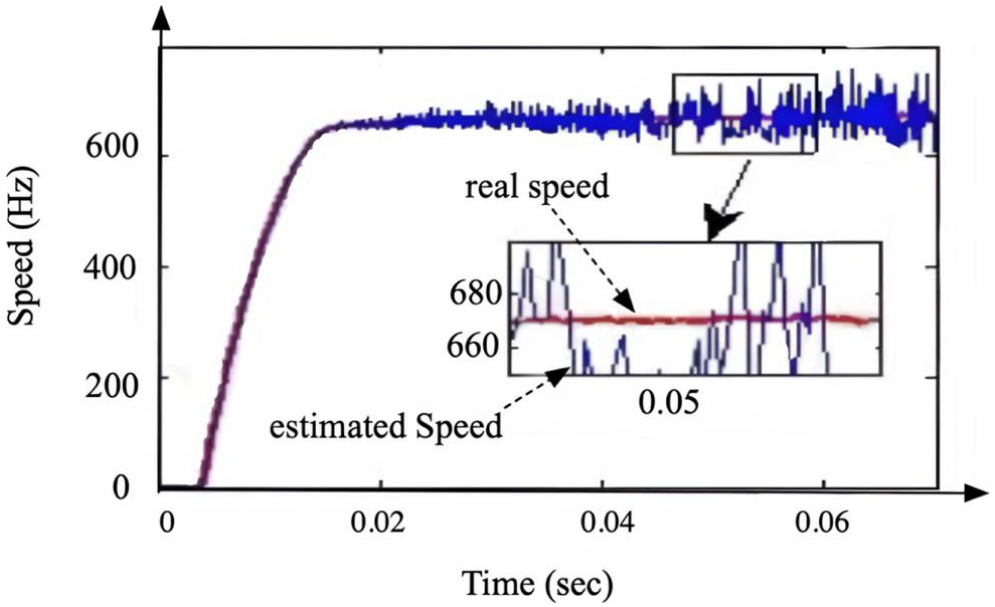

Fig. 11. Speed performance (HZ): red color: the real speed, blue color: the estimated speed

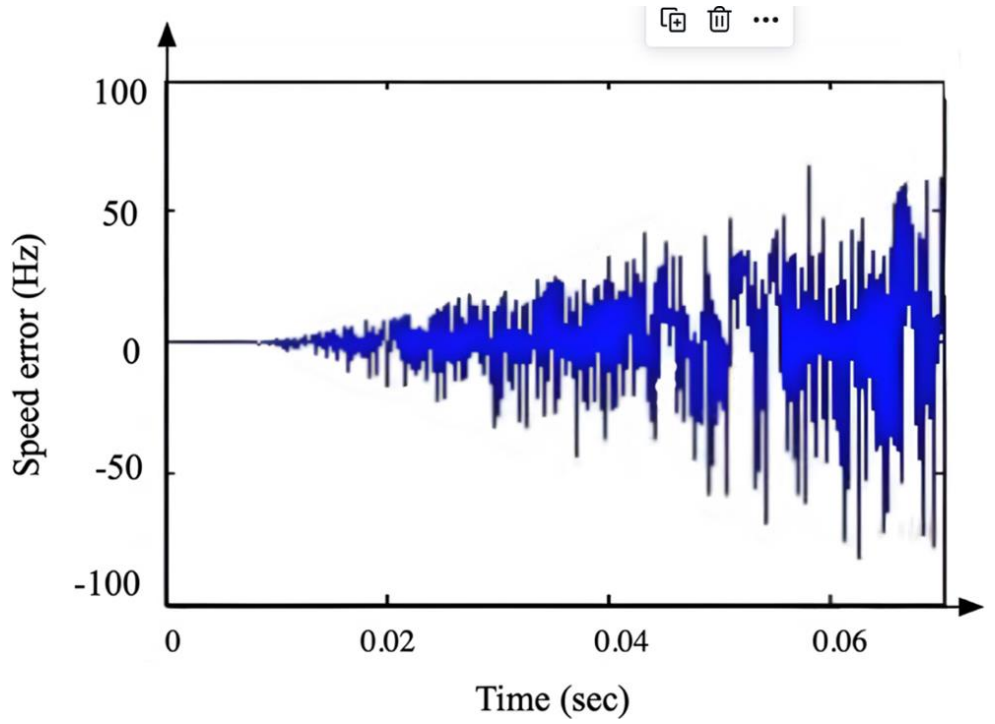

Fig. 12. Speed error between the real and esteemed MRAS speed

In this section the system running frequency is equivalent to 650 Hz; this large frequency variation has an impact on the commutation blocs inserted on the software speed encoder (the Sign Bloc inserted in Fig. 5); as a result, we see a lot of chatter at this frequency. We propose that this

software speed encoder version run at a maximum speed of 400 Hz. Fig. 12 depicts the speed error between the measured and estimated values. However, the system's robustness is not affected. These problems will take our research objective in future works.

7. Conclusion and Work Summary

This study uses PMSM control without a speed encoder. The Model Reference Adaptive System ensures the speed encoder after changing its PI controller using the PSO tool, which is based on reactive power characteristics. The vector control technique is employed to ensure motor control, and the High Speed Algorithm is used when operating in this mode. The selection of the speed observer is based on the robustness of the speed estimation tool phase and the motor parameters variation as the stator resistance. From the other side, and in relation to the specification of the wind system, which faces a high speeds regions due to high wind speed, the motor speed observer has to be efficient enough in that speed characterization.

The associated speed observer was created using the Matlab software tool and validated on an actual prototype that could function at 42K rpm. Based on the data, and for 600 hz, a maximum inaccuracy of 8.5% is calculated. In general, the suggested software speed encoder will be efficient in wind system models with wind speeds of less than 150 km/h.

Even the obtained results are accepted enough, it is mandatory to continue working on this observer by testing its specification on other motor parameters variations as the magnet flux level, which can also change due some external perturbation as temperature or vibration. In a second point of view, the proposed speed observer can be enough benefit for high-speed cars, which use the high speed mode (boost mode) in some cases, then it will be more easy in motor complexity and traction system prices. So testing this speed observer in traction system and triboelectric systems can have future endeavours of this proposed prototype for resolving some common problems.

In summary, this study introduces a robust high-speed estimator algorithm based on the Model Reference Adaptive System (MRAS) approach, which utilizes a reactive power model to maintain performance accuracy despite variations in stator resistance. The estimator was rigorously tested up to 42,000 RPM (600 Hz), demonstrating a maximum speed estimation error of 50 Hz. The results validate the estimator’s effectiveness and its potential to enhance speed detection in wind energy systems, contributing significantly to the domain by providing a solution to the challenges posed by high-speed operation and motor parameter variations. However, the study does have limitations, such as the reliance on a specific optimization algorithm and the use of a single prototype for validation.

8. Future Works

The related Future research should explore the application of alternative optimization techniques to further refine estimator performance and extend validation to a broader range of machine prototypes and operating conditions. Additionally, integrating advanced sensor technologies and real-time data processing could further improve the estimator’s accuracy and robustness. This research contributes new theoretical insights into the application of MRAS-based estimators in high-speed environments and offers practical advancements for wind energy systems. By addressing critical issues related to speed estimation at high velocities, this work paves the way for future innovations and encourages continued exploration in this area to enhance the reliability and efficiency of wind energy technologies.

Author Contribution: All authors contributed equally to the main contributor to this paper. All authors read and approved the final paper.

Acknowledgment: This study is supported via funding from Prince sattam bin Abdulaziz University project number (PSAU/2024/R/1446).

Conflicts of Interest: The authors declare no conflict of interest.

References

[1] F. Aymen and S. Lassâad, "Overview on BLAC and BLDC motors: designs and mathematical modeling," *International Journal of Powertrains*, vol. 10, no. 2, pp. 204-215, 2021, https://doi.org/10.1504/IJPT.2021.10040735.

[2] A. Swetapadma *et al*., "A novel primary and backup relaying scheme considering internal and external faults in HVDC transmission lines," *Frontiers in Energy Research*, vol. 10, p. 1003169, 2022, https://doi.org/10.3389/fenrg.2022.1003169.

[3] R. Kumar, S. Das, and A. K. Chattopadhyay, "Comparative assessment of two different model reference adaptive system schemes for speed-sensorless control of induction motor drives," *IET Electric Power Applications*, vol. 10, no. 2. pp. 141-154, 2016, https://doi.org/10.1049/iet-epa.2015.0121.

[4] G. Waltrich, J. L. Duarte and M. A. M. Hendrix, "Multiport Converter for Fast Charging of Electrical Vehicle Battery," *IEEE Transactions on Industry Applications*, vol. 48, no. 6, pp. 2129-2139, 2012, https://doi.org/10.1109/TIA.2012.2226694.

[5] M. Hwang, J. Han, D. Kim, and H. Cha, "Design and Analysis of Rotor Shapes for IPM Motors in EV Power Traction Platforms," *Energies*, vol. 11, no. 10, p. 2601, 2018, https://doi.org/10.3390/en11102601.

[6] A. Flah, M. Novak, and S. Lassaad, "An Improved Reactive Power MRAS Speed Estimator With Optimization for a Hybrid Electric Vehicles Application," *Journal of Dynamic Systems, Measurement, and Control*, vol. 140, no. 6, p. 061016, 2018, https://doi.org/10.1115/1.4039212.

[7] H. Hanene, F. Aymen, and T. Souhir, "Variable Reluctance Synchronous Machines in Saturated Mode," *International Journal of Power Electronics and Drive Systems*, vol. 12, no. 2, pp. 662-673, 2021, https://doi.org/10.11591/ijpeds.v12.i2.pp662-673.

[8] N. Al-Aawar and A. -R. A. Arkadan, "Optimal Control Strategy for Hybrid Electric Vehicle Powertrain," *IEEE Journal of Emerging and Selected Topics in Power Electronics*, vol. 3, no. 2, pp. 362-370, 2015, https://doi.org/10.1109/JESTPE.2014.2323019.

[9] V. Verma, C. Chakraborty, S. Maiti and Y. Hori, "Speed Sensorless Vector Controlled Induction Motor Drive Using Single Current Sensor," *IEEE Transactions on Energy Conversion*, vol. 28, no. 4, pp. 938-950, 2013, https://doi.org/10.1109/TEC.2013.2273935.

[10] S. Rind, Y. Ren and L. Jiang, "Traction motors and speed estimation techniques for sensorless control of electric vehicles: A review," *2014 49th International Universities Power Engineering Conference (UPEC)*, pp. 1-6, 2014, https://doi.org/10.1109/UPEC.2014.6934646.

[11] A. Flah, M. Novák, L. Sbita, J. Novák, "Estimation of motor parameters for an electrical vehicle application," *International Journal of Modelling, Identification and Control*, vol. 22, no. 2, pp. 150-158, 2014, https://doi.org/10.1504/IJMIC.2014.064290.

[12] F. Aymen, O. Berkati, S. Lassaad and M. N. Srifi, "BLDC Control Method Optimized by PSO Algorithm," *2019 International Symposium on Advanced Electrical and Communication Technologies (ISAECT)*, pp. 1-5, 2019, https://doi.org/10.1109/ISAECT47714.2019.9069718.

[13] N. Mohamed, F. Aymen, M. B. Hamed, S. Lassaad, "Analysis of Battery-EV state of charge for a Dynamic Wireless Charging system," *Energy Storage*, vol. 2, no. 2, p. e117, 2019, https://doi.org/10.1002/est2.117.

[14] L. N. Tutelea, I. Boldea and S. I. Deaconu, "Optimal design of dual rotor single stator PMSM drive for automobiles," *2012 IEEE International Electric Vehicle Conference*, pp. 1-8, 2012, https://doi.org/10.1109/IEVC.2012.6183224.

[15] H. Banvait, S. Anwar and Y. Chen, "A rule-based energy management strategy for Plug-in Hybrid Electric Vehicle (PHEV)," *2009 American Control Conference*, pp. 3938-3943, 2009, https://doi.org/10.1109/ACC.2009.5160242.

[16] J. Cheng, J. Cheng, M. Zhou, F. Liu, S. Gao and C. Liu, "Routing in Internet of Vehicles: A Review," *IEEE Transactions on Intelligent Transportation Systems*, vol. 16, no. 5, pp. 2339-2352, 2015, https://doi.org/10.1109/TITS.2015.2423667.

[17] R. B. A. Koad, A. F. Zobaa and A. El-Shahat, "A Novel MPPT Algorithm Based on Particle Swarm Optimization for Photovoltaic Systems," *IEEE Transactions on Sustainable Energy*, vol. 8, no. 2, pp. 468-476, 2017, https://doi.org/10.1109/TSTE.2016.2606421.

[18] A. Panday and H. Bansal, "A review of optimal energy management strategies for hybrid electric vehicle," *International Journal Vehicular Technology*, vol. 2014, no. 1, pp. 1-19, 2014, https://doi.org/10.1155/2014/160510.

[19] L. Sepulchre, M. Fadel, M. Pietrzak-David and G. Porte, "Flux-weakening strategy for high speed PMSM for vehicle application," *2016 International Conference on Electrical Systems for Aircraft, Railway, Ship Propulsion and Road Vehicles & International Transportation Electrification Conference (ESARS-ITEC)*, pp. 1-7, 2016, https://doi.org/10.1109/ESARS-ITEC.2016.7841413.

[20] D. G. Dorrell, M. -F. Hsieh, M. Popescu, L. Evans, D. A. Staton and V. Grout, "A Review of the Design Issues and Techniques for Radial-Flux Brushless Surface and Internal Rare-Earth Permanent-Magnet Motors," *IEEE Transactions on Industrial Electronics*, vol. 58, no. 9, pp. 3741-3757, 2011, https://doi.org/10.1109/TIE.2010.2089940.

[21] P. Gao, Y. Gu, and X. Wang, "The design of a permanent magnet in-wheel motor with dual-stator and dual-field-excitation used in electric vehicles," *Energies*, vol. 11, no. 2, p. 242, 2018, https://doi.org/10.3390/en11020424.

[22] A. Flah and L. Sbita, "A novel IMC controller based on bacterial foraging optimization algorithm applied to a high speed range PMSM drive," *Applied Intelligence*, vol. 38, pp. 114-129, 2013, https://doi.org/10.1007/s10489-012-0361-0.

[23] H. Wang, W. Sun, D. Jiang and R. Qu, "A MTPA and Flux-Weakening Curve Identification Method Based on Physics-Informed Network Without Calibration," *IEEE Transactions on Power Electronics*, vol. 38, no. 10, pp. 12370-12375, 2023, https://doi.org/10.1109/TPEL.2023.3295913.

[24] P. Pillay and R. Krishnan, "Modeling, simulation, and analysis of permanent-magnet motor drives. II. The brushless DC motor drive," *IEEE Transactions on Industry Applications*, vol. 25, no. 2, pp. 274-279, 1989, https://doi.org/10.1109/28.25542.

[25] M. Boufadene, "Modeling and Control of AC Machine using MATLAB®/SIMULINK," *CRC Press*, p. 70, 2018, https://doi.org/10.1201/9780429029653.

[26] S. Panda *et al*., "An Insight into the Integration of Distributed Energy Resources and Energy Storage Systems with Smart Distribution Networks Using Demand-Side Management," *Applied Science*, vol. 12, no. 17, p. 8914, 2022, https://doi.org/10.3390/app12178914.

[27] A. L. Facci, L. Andreassi, F. Martini, and S. Ubertini, "Comparing Energy and Cost Optimization in Distributed Energy Systems Management," *Journal Energy Resource Technology*, vol. 136, no. 3, pp. 32001-32009, 2014, https://doi.org/10.1115/1.4027155.

[28] J. Song, A. Mingotti, J. Zhang, L. Peretto and H. Wen, "Accurate Damping Factor and Frequency Estimation for Damped Real-Valued Sinusoidal Signals," *IEEE Transactions on Instrumentation and Measurement*, vol. 71, pp. 1-4, 2022, https://doi.org/10.1109/TIM.2022.3220300.

[29] J. Song, A. Mingotti, J. Zhang, L. Peretto and H. Wen, "Fast Iterative-Interpolated DFT Phasor Estimator Considering Out-of-Band Interference," *IEEE Transactions on Instrumentation and Measurement*, vol. 71, pp. 1-14, 2022, https://doi.org/10.1109/TIM.2022.3203459.

[30] J. Zhang *et al*., "Fractional Order Complementary Non-singular Terminal Sliding Mode Control of PMSM Based on Neural Network," *International Journal of Automotive Technology*, vol. 25, pp. 213-224, 2024, https://doi.org/10.1007/s12239-024-00015-9.

[31] B. Babes, N. Hamouda, S. Kahla, H. Amar, and S. S. M. Ghoneim, "Fuzzy model based multivariable predictive control design for rapid and efficient speed-sensorless maximum power extraction of renewable wind generators," *Electrical Engineering & Electromechanics*, no. 3, pp. 51-62, https://doi.org/10.20998/2074-272X.2022.3.08.

[32] N. Hamouda, B. Babes, S. Kahla and Y. Soufi, "Real Time Implementation of Grid Connected Wind Energy Systems: Predictive Current Controller," *2019 1st International Conference on Sustainable Renewable Energy Systems and Applications (ICSRESA)*, pp. 1-6, 2019, https://doi.org/10.1109/ICSRESA49121.2019.9182526.

[33] F. Aymen, S. Lassâad, "An improved PMSM drive architecture based on BFO and neural network," *International Journal of Advanced Robotic Systems*, vol. 10, no. 4, 2013, https://doi.org/10.5772/53011.

[34] Y. Hori, "Future vehicle driven by electricity and Control-research on four-wheel-motored "UOT electric march II"," *IEEE Transactions on Industrial Electronics*, vol. 51, no. 5, pp. 954-962, 2004, https://doi.org/10.1109/TIE.2004.834944.

[35] K. V. Singh, H. O. Bansal, and D. Singh, "A comprehensive review on hybrid electric vehicles: architectures and components," *Journal of Modern Transportation*, vol. 27, pp. 77-107, 2019, https://doi.org/10.1007/s40534-019-0184-3.

[36] J. Stefanovski, "Kalman–Yakubovič–Popov lemma for descriptor systems," *Systems & Control Letters*, vol. 74, pp. 8-13, 2014, https://doi.org/10.1016/j.sysconle.2014.08.015.

[37] B. Antar, B. Hassen, B. Babes and H. Afghoul, "Fractional order PI controller for grid connected wind energy conversion system," *2015 4th International Conference on Electrical Engineering (ICEE)*, pp. 1-6, 2015, https://doi.org/10.1109/INTEE.2015.7416692.

[38] R. Kumar, S. Das, and A. K. Chattopadhyay, "Comparison of Q- and X-MRAS for speed sensor less induction motor drive on," *Michael Faraday IET International Summit 2015*, pp. 319-324, 2015, https://doi.org/10.1049/cp.2015.1651.

[39] J. M. Miller, O. C. Onar and M. Chinthavali, "Primary-Side Power Flow Control of Wireless Power Transfer for Electric Vehicle Charging," *IEEE Journal of Emerging and Selected Topics in Power Electronics*, vol. 3, no. 1, pp. 147-162, 2015, https://doi.org/10.1109/JESTPE.2014.2382569.

[40] A. V. S. Reddy *et al*., "Power Quality Improvement in Integrated System using Inductive UPQC," *International Journal of Renewable Energy Research*, vol. 11, no. 2, pp. 566-576, 2021, https://dorl.net/dor/20.1001.1.13090127.2021.11.2.6.5.

[41] K. Itani, A. De Bernardinis, Z. Khatir, A. Jammal and M. Oueidat, "Regenerative Braking Modeling, Control, and Simulation of a Hybrid Energy Storage System for an Electric Vehicle in Extreme Conditions," *IEEE Transactions on Transportation Electrification*, vol. 2, no. 4, pp. 465-479, 2016, https://doi.org/10.1109/TTE.2016.2608763.

[42] A. P. Hu, C. Liu and H. L. Li, "A Novel Contactless Battery Charging System for Soccer Playing Robot," *2008 15th International Conference on Mechatronics and Machine Vision in Practice*, pp. 646-650, 2008, https://doi.org/10.1109/MMVIP.2008.4749606.

[43] H. El Fadil, F. Giri, J. M. Guerrero and A. Tahri, "Modeling and Nonlinear Control of a Fuel Cell/Supercapacitor Hybrid Energy Storage System for Electric Vehicles," *IEEE Transactions on Vehicular Technology*, vol. 63, no. 7, pp. 3011-3018, 2014, https://doi.org/10.1109/TVT.2014.2323181.

[44] M. Alam, K. Kumar, and V. Dutta, "Comparative efficiency analysis for silicon, silicon carbide MOSFETs and IGBT device for DC–DC boost converter," *SN Applied Sciences*, vol. 1, no. 12, pp. 1-11, 2019, https://doi.org/10.1007/s42452-019-1778-4.

[45] Y. Luo, C. Liu, F. Yu, and C. H. T. Lee, "Design & evaluation of an efficient three-phase four-leg voltage source inverter with reduced IGBTs," *Energies*, vol. 10, no. 4, p. 530, 2017, https://doi.org/10.3390/en10040530.

[46] T. M. Jahns *et al*., "Design and Experimental Verification of a 50 kW Interior Permanent Magnet Synchronous Machine," *Conference Record of the 2006 IEEE Industry Applications Conference Forty-First IAS Annual Meeting*, Tampa, pp. 1941-1948, 2006, https://doi.org/10.1109/IAS.2006.256801.

[47] K. Zhang, B. Jiang, X. -G. Yan and Z. Mao, "Incipient Fault Detection for Traction Motors of High-Speed Railways Using an Interval Sliding Mode Observer," *IEEE Transactions on Intelligent Transportation Systems*, vol. 20, no. 7, pp. 2703-2714, 2019, https://doi.org/10.1109/TITS.2018.2878909.

[48] L. Gong and C. Zhu, "Vibration Suppression for Magnetically Levitated High-Speed Motors Based on Polarity Switching Tracking Filter and Disturbance Observer," *IEEE Transactions on Industrial Electronics*, vol. 68, no. 6, pp. 4667-4678, 2021, https://doi.org/10.1109/TIE.2020.2989710.

[49] H. Kim, J. Son and J. Lee, "A High-Speed Sliding-Mode Observer for the Sensorless Speed Control of a PMSM," *IEEE Transactions on Industrial Electronics*, vol. 58, no. 9, pp. 4069-4077, 2011, https://doi.org/10.1109/TIE.2010.2098357.

[50] W. Xu, S. Qu, L. Zhao and H. Zhang, "An Improved Adaptive Sliding Mode Observer for Middle- and High-Speed Rotor Tracking," *IEEE Transactions on Power Electronics*, vol. 36, no. 1, pp. 1043-1053, 2021, https://doi.org/10.1109/TPEL.2020.3000785.

[51] J. Guzinski, H. Abu-Rub, M. Diguet, Z. Krzeminski and A. Lewicki, "Speed and Load Torque Observer Application in High-Speed Train Electric Drive," *IEEE Transactions on Industrial Electronics*, vol. 57, no. 2, pp. 565-574, 2010, https://doi.org/10.1109/TIE.2009.2029582.